SNX5 is essential for efficient macropinocytosis and antigen processing in primary macrophages

Jet Phey Lim[1], Rohan D. Teasdale[2] and Paul A. Gleeson[1,*]

[1]Department of Biochemistry and Molecular Biology, Bio21 Molecular Science and Biotechnology Institute, University of Melbourne, Victoria 3010, Australia
[2]Institute for Molecular Bioscience, University of Queensland, Brisbane, Queensland 4072, Australia
*Author for correspondence (pgleeson@unimelb.edu.au)

Biology Open 1, 904–914
doi: 10.1242/bio.20122204
Received 11th June 2012
Accepted 19th June 2012

Summary

Macropinocytosis mediates the bulk endocytosis of solute molecules, nutrients and antigens. As this endocytic pathway is considered important in functions associated with immune responses, the molecular mechanisms regulating this pathway in immune cells is of particular significance. However, the regulators of macropinocytosis in primary cells remain poorly defined. Members of the sorting nexin (SNX) family have been implicated in macropinosome biogenesis in cultured cells and here we have analyzed the role of two SNX family members, SNX1 and its binding partner SNX5, in macropinocytosis of mouse primary macrophages. We show that endogenous SNX1 and SNX5 are localised to newly-formed macropinosomes in primary mouse macrophages and, moreover, demonstrate that SNX5 plays an essential role in macropinosome biogenesis. Depletion of SNX5 in bone marrow-derived macrophages dramatically decreased both the number and size of macropinosomes. Depletion of SNX5 also resulted in dramatic reduction in uptake and processing of soluble ovalbumin in macrophages, indicating that the majority of antigen uptake and delivery to late endosomes is via macropinocytosis. By contrast, the absence of SNX1 had no effect on endogenous SNX5 localisation and macropinosome biogenesis using macrophages from SNX1 knockout mice. Therefore, SNX5 can function independently of SNX1 and is a modulator of macropinocytosis that influences the uptake and processing of soluble antigen in primary mouse macrophages.

Key words: Macropinocytosis, Sorting nexins, Endocytosis, Antigen processing, SNX5

Introduction

Macropinocytosis is an endocytosis pathway that arises from actin-mediated membrane ruffling of the plasma membrane. Macropinosomes are derived from lamellipodia which fold back on themselves and fuse with the basal membrane creating large, irregular shaped endocytic vesicles with a diameter > 0.2 μm to 10 μm (Hewlett et al., 1994; Swanson and Watts, 1995) and which lack coat structures. Given their large size compared with other endocytic processes, macropinosomes very efficiently mediate the bulk uptake of solute molecules, nutrients and antigens as well as considerable amounts of plasma membrane. A key difference between clathrin-dependent endocytosis and macropinocytosis is that the latter requires actin cytoskeleton reorganisation whereas the former is actin independent in many circumstances. Unlike clathrin-mediated endocytosis, macropinocytosis is regulated by the activation of receptor tyrosine kinases which occur in response to growth factor stimulation such as macrophage colony stimulating factor (CSF-1), epidermal growth factor (EGF) and platelet-derived growth factor (PDGF) or tumour promoting factor such as phorbol myristate acetate (PMA) (Dharmawardhane et al., 2000; Haigler et al., 1979; Racoosin and Swanson, 1989; Swanson, 1989). Some specialised cell types such as antigen presenting cells are capable of constitutive macropinocytosis (Norbury et al., 1997; Norbury et al., 1995; Sallusto et al., 1995).

The capacity of macropinocytosis to endocytose large quantities of extracellular fluid underpins a variety of functions in development, cell motility, tumour progression and metastasis (Carpentier et al., 1991), and also innate and adaptive immune responses. Some opportunistic pathogens such as the protozoa, bacteria, viruses and prions have exploited the macropinocytic pathway and its machineries to invade and evade the host immune system (Lim and Gleeson, 2011). In the immune system, antigen presenting cells such as the dendritic cells and macrophages utilise macropinocytosis as a major pathway for the capture of antigens from their immediate surrounding (Norbury et al., 1997; Norbury et al., 1995; Sallusto et al., 1995).

Given the physiological relevance of macropinocytosis, it is important to identify the regulatory components of this endocytic pathway. The downstream targets of phosphoinositide (PI) 3-kinase signalling, namely phosphoinositides, have been shown to be critical in the biogenesis of macropinosomes (Amyere et al., 2000; Anzinger et al., 2012; Araki et al., 1996; Clague et al., 1995; Kerr et al., 2010). Mapping of phosphoinositide derivatives during macropinocytosis has demonstrated a high level of PI(3,4,5)P_3 at the site of macropinosome formation and a rapid transition from PI(3,4,5)P_3 to PI(3)P as the macropinosome is closed (Yoshida et al., 2009). In addition, phosphoinositide effectors have been shown to be recruited to macropinosomes as

they form and mature (Kerr et al., 2010; Yoshida et al., 2009) and the recruitment of PI effectors are likely to regulate the process of macropinocytosis. One family of effectors which bind to phosphoinositides, and which are known to regulate membrane trafficking, are sorting nexins (SNXs), cytoplasmic and membrane associated proteins involved in various aspects of endocytosis and membrane trafficking (Cullen, 2008; Worby and Dixon, 2002). Members of the sorting nexin family are characterised by the presence of a phox (PX) domain, a sequence of approximately 70–110 residues that interacts with a variety of phosphoinositide species, especially PI(3)*P* (Teasdale et al., 2001; Xu et al., 2001). A subgroup of sorting nexins also contains long C-terminal coiled coil regions called BAR domains. The BAR domain promotes homo- and hetero-dimerization of the SNX-BAR proteins, and forms a crescent shaped structure which can associate with membranes to sense membrane curvature and to promote membrane tubulation (Peter et al., 2004). Over-expression of a number of SNX-BAR protein members have been shown to elevate macropinosome formation, in particular SNX1, SNX5, SNX9, SNX18 and SNX33 (Wang et al., 2010). Of relevance to the current study, SNX1 and SNX5, in particular, have been reported to exist as a heterodimers based on yeast two-hybrid analyses and analyses of transfected cells overexpressing these sorting nexins (Kerr et al., 2006; Liu et al., 2006; Wassmer et al., 2009).

We have previously demonstrated that the PI(3)*P* and PI(3,4)P_2 binding-SNX-BAR protein, SNX5 is involved early in the formation of macropinocytosis in cultured cells (Lim et al., 2008). SNX5 is transiently recruited to the plasma membrane after EGF receptor stimulation (Merino-Trigo et al., 2004) and this recruitment of SNX5 to the plasma membrane is dependent on elevated levels of PI(3,4)P_2 (Lim et al., 2008). After EGF stimulation of HEK293 cells, large SNX5-positive structures, which labelled with fluid phase markers, were detected in close proximity to membrane ruffles (Kerr et al., 2006). SNX5 localised to the macropinosome body and tubules that extended and departed from the newly-formed macropinosomes (Kerr et al., 2006). The extensive tubulation during macropinosome maturation is considered to provide a potential mechanism for rapid membrane and cargo protein recycling back to the plasma membrane for subsequent macropinocytic events. Significantly, SNX5 influences the level of macropinocytic activity as stable over-expression of SNX5 resulted in a 2-fold increase in macropinosome biogenesis (Lim et al., 2008). Based on these studies SNX5 has been proposed to play a role directly in the biogenesis of macropinosomes and/or in the maintenance of membrane flux between the plasma membrane and internalised macropinosomes by membrane recycling. Although informative, these studies involve overexpression of the sorting nexins and the relevance of SNX5 and SNX1/SNX5 dimers to the regulation of macropinocytosis in primary cells remains unclear.

Antigen presenting cells such as the dendritic cells and macrophages are considered to utilise macropinocytosis as a major pathway to capture antigens (Norbury et al., 1997; Norbury et al., 1995; Sallusto et al., 1995), which are processed and antigenic peptides loaded onto MHC molecules for presentation to T-cells. Macrophages have been shown to undergo constitutive macropinocytosis (Steinman et al., 1976). More extensive analyses of macropinocytosis pathways in primary cells are necessary for translation of the findings to the whole organism. In particular, the identification of macropinosome regulators in primary immune cells would provide a significant advance in the field as it would allow the opportunity to investigate the precise roles of macropinocytosis by antigen presenting cells *in vitro* and *in vivo*. Here we have investigated the role of endogenous SNX1 and SNX5 in macropinocytosis and antigen processing in primary macrophages. Our findings demonstrate that SNX5, but not SNX1, regulates macropinocytosis, antigen uptake and ultimately levels of antigen processing in primary macrophages.

Results

SNX1-deficient macrophages are not affected in the biogenesis of macropinocytosis

The identification of regulators of macropinosome biogenesis in immune cells is an important prerequisite to establish the contribution of macropinocytosis to antigen processing and presentation. Given the known key roles of sorting nexins in membrane trafficking (Carlton et al., 2005), and their association with macropinosomes in different cell types (Bryant et al., 2007; Kerr et al., 2006; Lim et al., 2008; Merino-Trigo et al., 2004), initially we examined macrophages from $SNX1^{-/-}$ mice. $SNX1^{-/-}$ mice (Schwarz et al., 2002) were obtained from the Mutant Mouse Regional Resource Centre (USA) and the genotypes verified, as described (Schwarz et al., 2002). Bone-marrow derived macrophages (BMM) were generated as large numbers of cells could be readily obtained. No SNX1 staining was observed in BMM from $SNX1^{-/-}$ mice compared with cells from $SNX1^{+/+}$ mice (data not shown) verifying that cells from $SNX1^{-/-}$ mice are indeed SNX1-deficient.

BMM were generated from 8–10 week old $SNX1^{+/+}$ and $SNX1^{-/-}$ littermate mice and the biogenesis of macropinosomes assessed. BMM were incubated with FITC-conjugated 70 kDa dextran in the presence of CSF-1 for 15 min at 37℃, or on ice as control, and macropinosomes identified as FITC-70 kDa dextran-labelled structures >500 nm in diameter. No significant difference in the number of macropinosomes per cell between BMM from $SNX1^{-/-}$ and $SNX1^{+/+}$ mice was observed in two independent experiments (Table 1). Similar results were obtained with peritoneal macrophages from $SNX1^{+/+}$ and $SNX1^{-/-}$ mice (data not shown). Therefore, the absence of SNX1 had no apparent effect on macropinosome biogenesis.

Localization of SNX1 and SNX5 on macropinosomes in primary mouse macrophages

Given the finding that SNX1 deficiency has no effect on macropinocytosis in macrophages, we therefore investigated the localisation of endogenous SNX1 and its binding partner, SNX5, to ascertain the relationship of these sorting nexins with newly formed macropinosomes in these primary cells. To label

Table 1. Absence of SNX1 does not affect macropinosome biogenesis in bone marrow-derived macrophages. BMM were incubated with FITC-conjugated 70 kDa dextran in the presence of CSF-1 for 15 min at 37℃ and the macropinosomes enumerated as described in Materials and Methods.

		Mean number of macropinosomes per cell ± SD
Experiment 1	$SNX1^{+/+}$	12.76 ± 5.97
	$SNX1^{-/-}$	11.48 ± 3.83
Experiment 2	$SNX1^{+/+}$	12.64 ± 4.51
	$SNX1^{-/-}$	14.32 ± 6.26

macropinosomes, primary peritoneal macrophages were incubated with FITC-conjugated 70 kDa dextran at 37℃ for 15 min. After 15 min, 70 kDa dextran labelled predominantly "donut-like" large structures and also to a lesser extent smaller endosomal structures (Fig. 1A,B). The donut appearance arises from the association of the fixable dextran with biomolecules associated with the membranes of the macropinosomes and the loss of non-fixed, luminal, dextran during permeabilization steps. The majority of the 70 kDa dextran-labelled "donut-like" structures were >500 nm in diameter (Fig. 1A,B), a size compatible with classical macropinosomes. Moreover, the 70 kDa dextran-labeled "donut-like" structures observed in paraformaldehyde-fixed peritoneal macrophages were reduced in number by >95% in cells treated with the selective macropinosome inhibitor, 5-(N-ethyl-N-isopropyl) amiloride (Koivusalo et al., 2010; West et al., 1989), confirming their identity (data not shown).

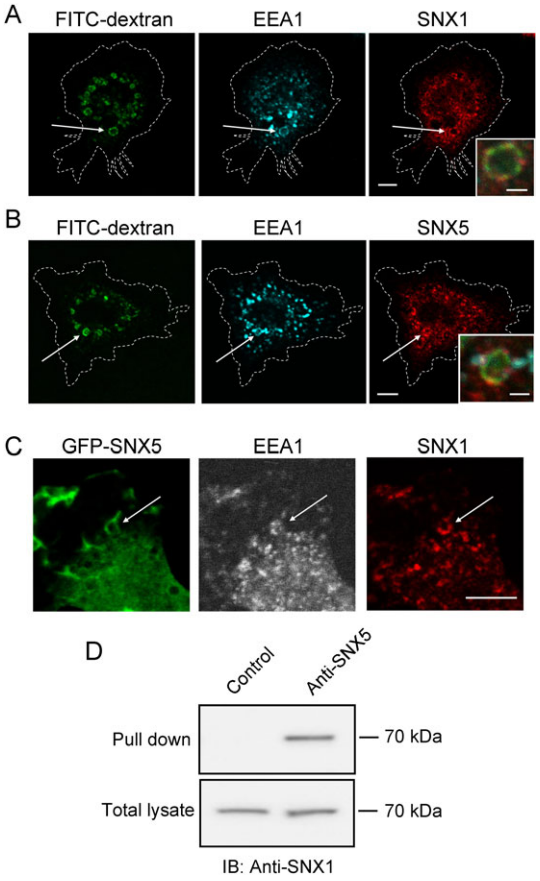

Fig. 1. SNX1 and SNX5 are localized on newly-formed macropinosomes. (**A–C**) Peritoneal macrophages from BALB/c mice were incubated with 500 µg/ml of FITC-conjugated 70 kDa dextran for 15 min at 37℃ to label newly-formed macropinosomes. Cells were then fixed in 4% paraformaldehyde, permeabilised, and stained with (A) human anti-EEA1 antibodies followed by Alexa 647-conjugated anti-human IgG and rabbit anti-SNX1 antibodies followed by Alexa 568-conjugated anti-rabbit IgG or (B) human anti-EEA1 antibodies followed by Alexa 647-conjugated anti-human IgG and rabbit anti-SNX5 antibodies followed by Alexa 568-conjugated anti-rabbit IgG. In (C) GFP-SNX5 was introduced into peritoneal macrophages from BALB/c mice by recombinant adenovirus, cells were fixed in 4% paraformaldehyde 24 hours after transduction and stained with rabbit anti-SNX1 antibodies followed by Alexa 568-conjugated anti-rabbit IgG and human anti-EEA1 antibodies followed by Alexa 647-conjugated anti-human IgG. EEA1 staining is shown in grey. Macropinosome indicated by arrows. Bars = 5 µm. For A and B macropinosomes indicated by an arrow are magnified in the insets. Bar of insets = 1 µm. (**D**) Peritoneal macrophages from BALB/c mice were lysed, incubated with rabbit anti-SNX5 IgG or normal rabbit IgG (control) and immune complexes precipitated with protein G Sepharose. Bound immune complexes, and total cell lysate, were resolved in a 10% NuPAGE® gel. Proteins were then transferred onto a PVDF membrane and probed with rabbit anti-SNX1 antibodies followed by HRP-conjugated anti-rabbit IgG. Bound antibodies were detected using chemiluminescence.

Primary peritoneal macrophages were incubated with FITC-conjugated 70 kDa dextran at 37℃ for 15 min and then stained for endogenous SNX1 and SNX5 using antibodies we generated to these mouse SNXs (Materials and Methods; supplementary material Fig. S3). Newly-formed macropinosomes >500 nm in diameter stained strongly for both endogenous SNX1 and SNX5 (Fig. 1A,B). The early endosome marker, EEA1, which has shown to be also a marker of newly-formed macropinosomes in cultured cells (Kerr et al., 2006; Merino-Trigo et al., 2004), was detected on the FITC-dextran labelled macropinosomes in peritoneal macrophages. Both SNX1 and SNX5 juxtaposed with EEA1 on boundary of the macropinosomes (Fig. 1A,B).

We then assessed whether both SNX1 and SNX5 were co-localised on the same macropinosomes or whether they may label distinct subpopulations. As co-staining with the rabbit anti-SNX1 and anti-SNX5 antibodies could not be performed, peritoneal macrophages were transduced with recombinant adenovirus encoding green fluorescent protein (GFP)-SNX5 and stained for EEA1 and SNX1. For this analysis, macropinosomes were identified based on their size (>500 nm diameter), circular structure and the staining pattern for EEA1 which resembled a halo. Despite a high background due to cytosolic GFP-SNX5, the analysis showed that GFP-SNX5 and SNX1 were localised on the same macropinosome structures juxtaposing with EEA1 (Fig. 1C). Collectively, these data indicate that both SNX1 and SNX5 are recruited to the same population of newly formed macropinosomes in primary mouse macrophages.

SNX1 and SNX5 have been reported to physically interact, based on yeast two-hybrid analyses and biochemical assays of transfected cells overexpressing sorting nexins (Kerr et al., 2006; Liu et al., 2006; Wassmer et al., 2009). Using the reagents we had generated, we investigated whether endogenous SNX1 and SNX5 in mouse primary macrophages can exist as a heterodimer. Peritoneal macrophages were isolated from BALB/c mice, lysed and endogenous SNX5 immunoprecipitated using anti-SNX5 antibodies. The immunoprecipitated complex was then analysed by immunoblotting for endogenous SNX1. The 70 kDa endogenous SNX1 co-immunoprecipitated with endogenous SNX5 (Fig. 1D). SNX1 was not detected in the control immunoprecipitation (Fig. 1D) demonstrating that the interaction was specific. A SNX1/SNX5 interaction was also detected by immunoprecipitation from bone-marrow derived macrophages (BMM) and NIH3T3 cells (data not shown). These data confirm that endogenous SNX1 and SNX5 can interact *in vivo* in primary cells and is consistent with the presence of a heterodimer.

We have previously demonstrated that elevated levels of SNX5 results in enhanced macropinocytic activity (Lim et al., 2008). Given the finding that SNX1 deficiency does not perturb macropinocytosis, and that SNX1 and SNX5 physically interact in primary macrophages, we assessed the level and localization of SNX5 in SNX1-deficient macrophages. Immunoblotting revealed that endogenous SNX5 was present at a similar level in BMM

from *SNX1*$^{+/+}$ and *SNX1*$^{-/-}$ mice, and furthermore, SNX5 was localized to both small and large (>500 nm diameter) EEA1-positive structures in SNX1-deficient BMM (Fig. 2). These results indicate that the absence of SNX1 does not affect the localization of SNX5 to endosomal and macropinosomal membranes in macrophages. Therefore, the removal of SNX5, or both SNX1 and SNX5, may be required to have an impact on macropinocytic activity.

Depletion of SNX5 in primary macrophages

To determine the influence of SNX5 in macropinocytosis in macrophages, we examined the effect of silencing SNX5 using the BLOCK-IT™ Pol II miR RNAi expression system. Out of five RNAi targets examined by immunofluorescence, SNX5 miRNA-1 was the optimum RNAi; however, SNX5 miRNA-1 reduced the level of SNX5 by only 40% as determined by immunoblotting (Fig. 3A). To further improve the efficiency of SNX5 depletion, a recombinant advenovirus construct with 4 copies of miRNA-1 in one primary transcript was generated, designated miRNA-1.4. Transduction of NIH3T3 cells with the recombinant SNX5 miRNA-1.4 adenovirus showed ~100% transduction efficiency (data not shown) and the level of SNX5 in NIH3T3 cells was reduced by ~ 92% compared to control miRNA (Fig. 3B,C).

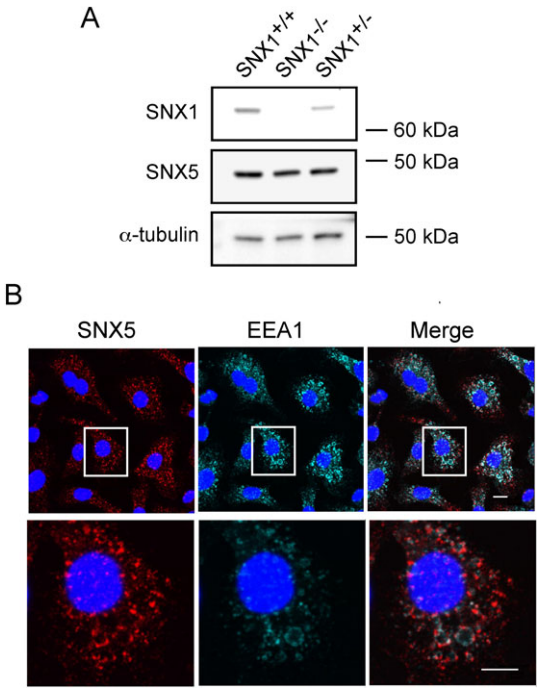

Fig. 2. Absence of SNX1 does not affect the level and localization of SNX5. (**A**) BMM from *SNX1*$^{+/+}$, *SNX1*$^{+/-}$ and *SNX1*$^{-/-}$ mice were lysed in reducing sample buffer and proteins resolved in a 10% NuPAGE® gel. Proteins were then transferred onto a PVDF membrane and probed with affinity-purified rabbit anti-SNX1 or anti-SNX5 antibodies followed by HRP-conjugated anti-rabbit IgG. Anti-SNX5 antibodies were stripped from the membrane to allow subsequent incubation with mouse monoclonal anti-α-tubulin antibodies followed by HRP-conjugated anti-mouse IgG. Bound antibodies were detected using chemiluminescence. (**B**) BMM from *SNX1*$^{-/-}$ mice were fixed in 4% paraformaldehyde, permeabilised, and stained with rabbit anti-SNX5 antibodies followed by Alexa 558-conjugated anti-rabbit IgG and anti-EEA1 antibodies followed by Alexa 647-conjugated anti-human IgG. Magnification of boxed region is shown in the bottom panel of B. Bars = 5 μm.

To determine if SNX5 miRNA-1.4 was able to silence SNX5 in peritoneal macrophages, BMM were transduced with the recombinant adenovirus and cells analysed 96 hours after transduction. Unfortunately, GFP+ transduced BMM had a similar level of SNX5 compared to the untransduced, wild-type (GFP-negative) cells (data not shown). Likewise peritoneal macrophages showed no reduction in SNX5 after transduction with SNX5 miRNA-1.4 adenovirus (data not shown). On the other hand, expression of an unrelated miRNA (GCC185 miRNA) in peritoneal macrophages showed effective silencing of GCC185 (not shown), demonstrating that the miRNA vector was functional in BMM.

SNX5 expression has been reported to be lower in hematopoietic stem cells than committed progenitor cells (Eckfeldt et al., 2005). As the silencing of SNX5 may be more efficient in hematopoietic stem cells we therefore introduced the SNX5 miRNA into hematopoietic progenitor bone marrow stem cells, prior to differentiation into macrophages. Hematopoietic progenitor bone marrow stem cells from BALB/c mice were

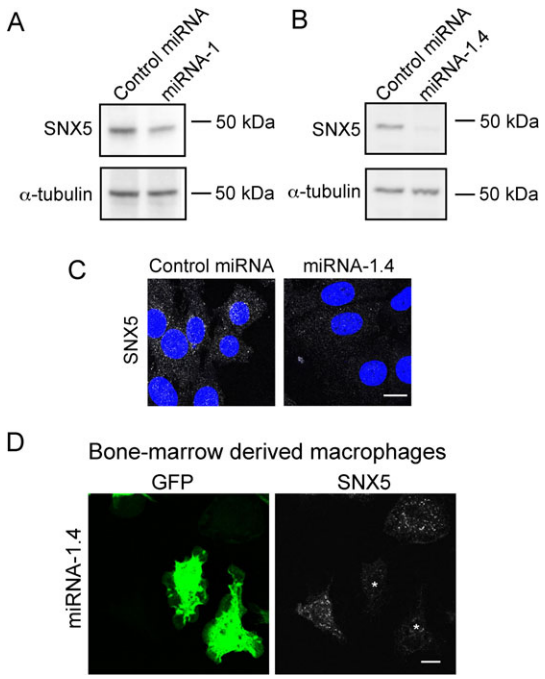

Fig. 3. SNX5 knockdown in NIH3T3 and primary macrophages. (**A**) NIH3T3 cells were transfected with control miRNA or miRNA-1, GFP+ cells sorted 96 hours later and then lysed in reducing sample buffer. (**B**) NIH3T3 cells were transduced with control miRNA or miRNA-1.4 recombinant adenovirus, and 96 hours later lysed in reducing sample buffer. (A,B) Proteins were resolved in a 10% NuPAGE® gel, transferred onto a PVDF membrane and probed with rabbit anti-SNX5 antibodies followed by HRP-conjugated anti-rabbit IgG. Rabbit anti-SNX5 antibodies were stripped from the membrane to allow subsequent incubation with mouse monoclonal anti-α-tubulin antibodies followed by HRP-conjugated anti-mouse IgG. Bound antibodies were detected using chemiluminescence. (**C**) NIH3T3 were fixed in 4% paraformaldehyde and permeabilised 72 hour after transduction and stained with rabbit anti-SNX5 antibodies followed by Alexa 568-conjugated anti-rabbit IgG. (**D**) miRNA-1.4 was introduced into progenitor bone marrow stem cells from BALB/c mice by recombinant adenovirus. Transduced stem cells were then differentiated into bone marrow-derived macrophages by culturing in the presence of CSF-1, fixed in 4% paraformaldehyde, permeabilised, and stained with rabbit anti-SNX5 antibodies followed by Alexa 568-conjugated anti-rabbit IgG. Asterisks (*) indicate transduced macrophages with reduced SNX5 expression. Bars = 10 μm.

transduced with SNX5 miRNA recombinant adenovirus and the cells cultured in the presence of CSF-1 for 72 hours to generate bone marrow-derived macrophages. The majority (65%) of bone marrow-derived macrophages were GFP-positive indicating that miRNA-1.4 was successfully introduced into the cells. The cells were positive for the macrophage marker, F4/80+, and had the decisive characteristics of bone marrow-derived macrophages (data not shown). Therefore, the expression of the miRNA construct did not influence macrophage differentiation. Two distinct populations were observed when GFP-positive BMM were stained for SNX5. Approximately 50% of the GFP-positive cells showed a dramatic reduction in SNX5 staining (Fig. 3D) while the remaining 50% of the GFP-positive cells showed normal levels of SNX5 staining. This result was reproducible in more than 5 separate experiments. Quantitative analysis of the SNX5 staining intensity indicated that the SNX5-silenced population of GFP+ BMM had SNX5 levels reduced by 89% compared with control BMM. Although the reason why only 50% of the GFP+ cells are effectively silenced in SNX5 is not clear, this strategy provided primary macrophages depleted in SNX5.

Depletion of SNX5 influences macropinocytosis

To investigate the physiological relevance of SNX5 in macropinocytosis, progenitor bone marrow stem cells from BALB/c mice were transduced with either miRNA-1.4 or control miRNA recombinant adenovirus, then differentiated into BMM by culturing in the presence of CSF-1. BMM, stimulated with 50 ng/ml CSF-1, were incubated with Texas Red (TxR)-conjugated 70 kDa dextran at 37℃ for 15 min to label newly-formed macropinosomes, identified as TxR- dextran-positive structures >500 nm in diameter. Cells were fixed and stained with anti-SNX5 antibodies to identify cells with reduced SNX5. BMM depleted of SNX5 had significantly reduced uptake of TxR-conjugated 70 kDa dextran (Fig. 4B) compared to BMM expressing control miRNA (Fig. 4A). To quantify the impact of SNX5 depletion on macropinocytosis, the mean number of TxR-dextran labelled macropinosomes per cell was determined for BMM expressing control miRNA and miRNA-1.4 with low levels of SNX5. BMM depleted of SNX5 showed a 60% reduction ($P<0.001$) in number of macropinosomes compared to cells expressing control miRNA (Fig. 4C). This result was reproducible (Table 2). The data were also analysed according to the number of macropinosomes per cell (Fig. 4D; Table 2). For cells depleted of SNX5, the majority of BMM (60%) had <6 macropinosomes per cell and none had >16 macropinosomes per cell (Table 2). In comparison, all cells expressing control miRNA had 6 or more macropinosomes per cell and > 40% of cells had 16 or more macropinosomes per cell (Table 2). Therefore, there was a dramatic reduction in the formation of macropinosomes in SNX5-depleted cells. A duplicate experiment showed reproducible distribution pattern in the number of macropinosomes formed per cell (Table 2).

In addition to the reduced number of macropinosomes, depletion of SNX5 resulted in the formation of smaller macropinosomes. The size of macropinosomes in either untransduced BMM (data not shown) or BMM expressing control miRNA can be up to ~4 µm in diameter (Fig. 4A). In BMM depleted of SNX5, the majority of macropinosomes were considerably smaller, ~1–2 µm in diameter (Fig. 4B). Collectively, the data show a reduced level of SNX5 affects not only macropinocytic activity but also the size of macropinosomes formed.

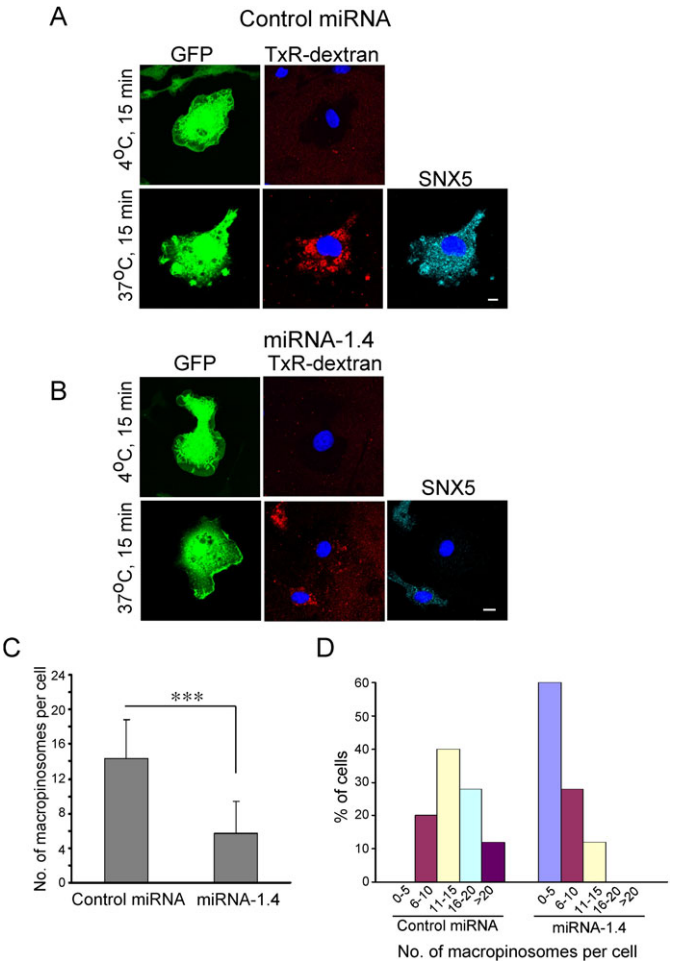

Fig. 4. Reduced levels of SNX5 affect macropinosome biogenesis in bone marrow derived macrophages. Progenitor bone marrow cells were transduced with control miRNA or miRNA-1.4 recombinant adenovirus and cells differentiated into BMM by culturing in the presence of CSF-1. After 72 hours, BMM were rendered quiescent by culturing overnight in complete RPMI and then incubated with 50 ng/ml CSF and 500 µg/ml TxR-conjugated 70 kDa dextran for 15 min at 37℃ or on ice. BMM were then fixed in 4% paraformaldehyde, permeabilised, and stained with rabbit anti-SNX5 antibodies followed by Alexa 647-conjugated anti-rabbit IgG. Macropinosomes were identified as TxR-conjugated 70 kDa dextran-positive structures of >500 nm in diameter. (**A**,**B**) Immunofluorescence images of cells. Bars = 5 µm. (**C**) The number of macropinosomes per cell for 25 cells was counted for each condition. Shown is the mean, and error bars represent standard deviation. *** P<0.001. (**D**) Percentage of cells with indicated number of macropinosomes per cell.

To eliminate the possibility of off-target effects of SNX5 miRNA-1.4, a second independent miRNA target sequence was identified, miRNA-2, and a multiple target copy of this target sequence, miRNA-2.4 reduced the level of endogenous SNX5 in NIH3T3 cells by 83% (supplementary material Fig. S1). BMM expressing miRNA-2.4 and depleted of SNX5 showed 50–60% decrease ($P<0.001$) in macropinocytosis compared to cells expressing control miRNA (Table 2). Silencing using miRNA-2.4 resulted in a similar decrease in number of macropinosomes per cell as for miRNA-1.4 (Table 2).

Depletion of SNX5 in *SNX1*$^{-/-}$ BMM

Although SNX1-deficiency does not influence macropinosome biogenesis in BMM, given the association of SNX1 and SNX5,

Table 2. Reduced levels of SNX5 affect macropinosome biogenesis in bone marrow-derived macrophages. Bone marrow stem cells were transduced with either control miRNA or SNX5 miRNA recombinant adenovirus, then differentiated into BMM. BMM were incubated with TxR-conjugated 70 kDa dextran in the presence of CSF-1 for 15 min at 37℃ and the macropinosomes enumerated in GFP+ cells as described in Materials and Methods.

Target sequence 1: miRNA-1.4							
			Distribution of number of macropinosomes per cell (%)				
		Mean number of macropinosomes per cell ± SD	0–5	6–10	11–15	16–20	> 20
Experiment 1	Control miRNA	14.28 ± 4.60	0	20	40	28	12
	miRNA-1.4	5.64 ± 3.83	60	28	12	0	0
Experiment 2	Control miRNA	15.92 ± 6.40	0	16	36	20	28
	miRNA-1.4	5.99 ± 4.87	48	32	12	8	0
Target sequence 2: miRNA-2.4							
			Distribution of number of macropinosomes per cell (%)				
		Mean number of macropinosomes per cell ± SD	0–5	6–10	11–15	16–20	> 20
Experiment 1	Control miRNA	14.12 ± 6.16	4	24	28	32	12
	miRNA-2.4	5.73 ± 3.44	52	40	4	4	0
Experiment 2	Control miRNA	13.96 ± 6.46	8	24	24	28	16
	miRNA-2.4	7.04 ± 4.02	48	36	12	4	0

depletion of both SNX1 and SNX5 may have a greater impact on macropinocytosis than SNX5 depletion alone. To investigate this possibility, SNX5 was silenced in *SNX1*$^{-/-}$ BMDM using SNX5 miRNA-1.4. Progenitor bone marrow stem cells from 8–10 week old *SNX1*$^{-/-}$ mice were either left untransduced or transduced with miRNA-1.4 or the control miRNA using recombinant adenoviruses. Transduced cells were then differentiated into BMM and then incubated with TxR-70 kDa dextran in the presence of 50 ng/ml CSF-1 stimulation to label newly-formed macropinosomes. *SNX1*$^{-/-}$ BMM depleted of SNX5 showed a ~50% reduction in macropinocytosis compared to untransduced cells or cells expressing control miRNA (supplementary material Fig. S2). The level of macropinocytosis between untransduced and cells expressing control miRNA were similar, indicating that macropinocytosis was unaffected by adenovirus transduction (supplementary material Fig. S2). In untransduced *SNX1*$^{-/-}$ BMM and *SNX1*$^{-/-}$ BMM expressing control miRNA, the majority of the cells (> 80%) had between 6–15 macropinosomes per cell. In contrast, very few (4%) of *SNX1*$^{-/-}$ BMDM depleted of SNX5 had >10 macropinosomes per cell (supplementary material Fig. S2). Therefore the absence of both SNX1 and SNX5 did not have a greater impact on the reduction of macropinocytosis than the depletion of SNX5 alone. Collectively, the data show that SNX5, and not SNX1, is the main modulator of macropinocytosis in BMM.

Influence of SNX1 and SNX5 on antigen (ovalbumin) uptake and processing by macrophages

To investigate the relevance of macropinocytosis on the uptake of soluble antigen, BMM were incubated with a mixture of FITC-70 kDa dextran and Alexa555-ovalbumin for 30 min at 37℃, or on ice as control. Alexa555-ovalbumin was detected in dextran-positive macropinosomes (Fig. 5A). As expected, neither dextran nor ovalbumin was internalised when the cells were incubated on ice (Fig. 5A). After 30 min internalisation, some of the ovalbumin-positive punctate structures stained positive for LAMP-1 (Fig. 5B), indicating the delivery of ovalbumin to the late endosome/lysosomes.

Processing of soluble antigen in acidic endosomal compartments is required for antigen presentation. To further explore the role of macropinocytosis in ovalbumin uptake and processing, DQ-ovalbumin was used as it has intrinsic fluorescent properties after exposure to a processing compartment. DQ-ovalbumin is a self-quenched conjugate of ovalbumin that exhibits fluorescence upon proteolytic degradation and can be used to study antigen uptake and processing in the late endosome/lysosome (Daro et al., 2000; Santambrogio et al., 1999). A 3 min pulse of BMM with DQ-ovalbumin followed by a 30 min chase resulted in the gradual increase in fluorescence at 615 nm,

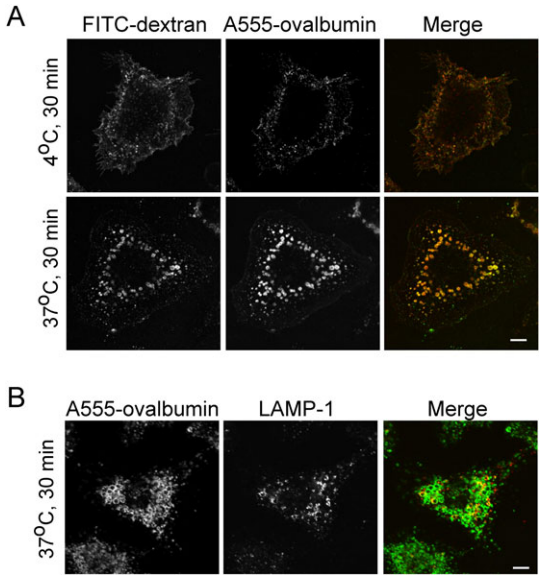

Fig. 5. Ovalbumin is internalized into LAMP-1 positive macropinosomes. BMM were rendered quiescent by culturing overnight in complete RPMI. The next day (**A**) BMM were incubated with 500 µg/ml of FITC-conjugated 70 kDa dextran and 50 µg/ml of Alexa 555-conjugated ovalbumin for 30 min at 37℃ or on ice in the presence of 50 ng/ml CSF-1 and then fixed in 4% paraformaldehyde. In (**B**) BMM were incubated with 50 µg/ml of Alexa 555-conjugated ovalbumin for 30 min at 37℃ and then fixed in methanol and stained with rat anti-LAMP-1 antibodies followed by Alexa 488-conjugated anti-rat IgG. FITC-dextran, Alexa 555-conjugated ovalbumin and LAMP-1 are shown in grey. Bars = 5 µm.

indicative of the processing of the DQ-ovalbumin by proteases in MHCII loading compartments (Fig. 6A). To determine the role of SNX5 on ovalbumin processing, progenitor bone marrow stem cells from BALB/c mice were transduced with either miRNA-1.4 or control miRNA recombinant adenovirus and then differentiated into bone marrow-derived macrophages as previously. BMM were then pulsed with DQ-ovalbumin for 3 min and chased in the presence of 50 ng/ml CSF-1 at 37℃ for 30 min, the time required for ovalbumin to reach LAMP-1 positive compartments. As a control, cells were continuously incubated in DQ-ovalbumin on ice. To identify cells with reduced SNX5 expression, fixed cells were stained with anti-SNX5 antibodies. BMM depleted of SNX5 have significantly reduced DQ-ovalbumin intensity as determined by immunofluorescence analysis (Fig. 6C) compared to BMM expressing control miRNA (Fig. 6B). Quantitative analyses showed a 60% reduction ($P<0.001$) in DQ-ovalbumin fluorescent intensity in SNX5-depleted BMM compared with control (Fig. 7A). The level of reduction in DQ-ovalbumin intensity is similar to the reduction in macropinosome biogenesis after SNX5 depletion (Fig. 4C), indicating that SNX5 is regulating antigen uptake and processing in primary macrophages. In contrast, no reduction in DQ-ovalbumin fluorescent intensity was observed in $SNX^{-/-}$ deficient BMM (Fig. 7B), indicating that SNX1 is not required for antigen uptake and processing. Therefore, these data show that SNX5 is a major regulator of antigen uptake and processing by primary macrophages.

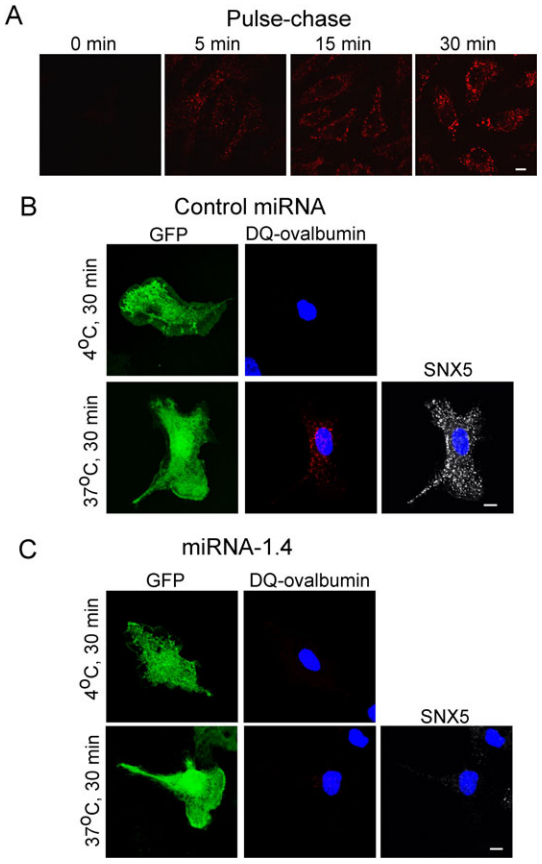

Fig. 6. SNX5 is required for DQ-ovalbumin uptake and processing. (**A**) Time course of DQ-ovalbumin processing by BMM. BMM were pulsed with DQ-ovalbumin for 3 min, washed and chased for time periods indicated in the presence of CSF-1. Bar = 10 µm. (**B**,**C**) Control miRNA or miRNA-1.4 was introduced into progenitor bone marrow cells from BALB/c mice by recombinant adenovirus. Cells were then differentiated into bone marrow-derived macrophages (BMM) by culturing in the presence of CSF-1. After 72 hours, BMM were rendered quiescent by culturing overnight in complete RPMI. The following day, BMM were pulsed with 50 µg/ml of DQ-ovalbumin for 3 min and chased in the presence of CSF-1 for 30 min at 37℃. A control was performed as a continuous incubation with DQ-ovalbumin in the presence of CSF-1 for 30 min on ice. BMM were then fixed in 4% paraformaldehyde, permeabilised, and stained with rabbit anti-SNX5 antibodies followed by Alexa 647-conjugated anti-rabbit IgG. Bars = 5 µm.

Discussion

Primary macrophages undergo a very high rate of constitutive macropinocytosis and represent an excellent cell type to identify the regulators of this pathway in specialised cells of the immune system (Tsang et al., 2000). Microarray data have indicated that

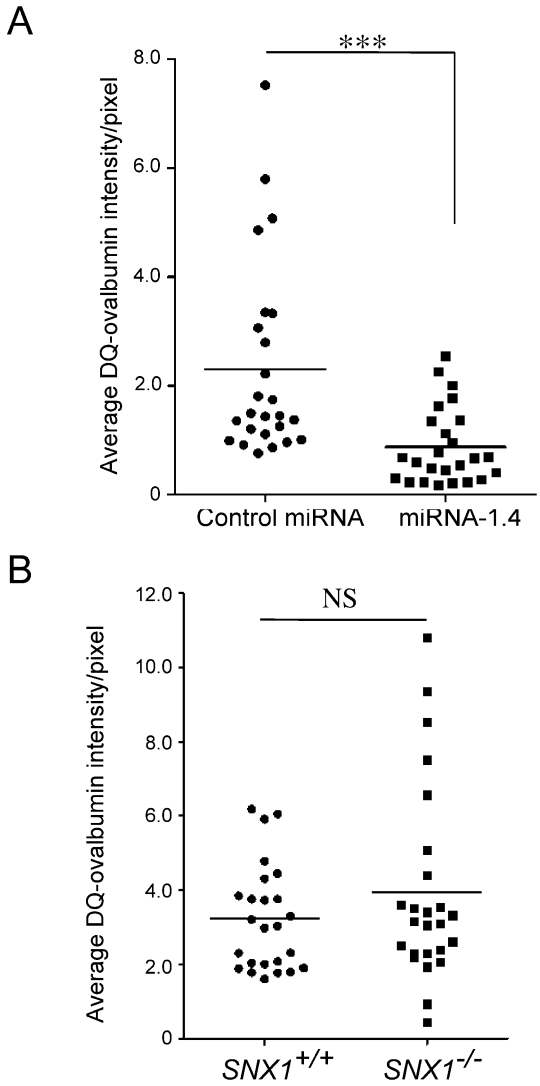

Fig. 7. Quantitation of DQ-ovalbumin processing in SNX5− and SNX1− deficient macrophages. (**A**) BMM expressing control and miRNA-1.4 and (**B**) BMM from $SNX1^{+/+}$ and $SNX1^{-/-}$ mice were cultured in the presence of CSF-1 and were pulsed with 50 µg/ml of DQ-ovalbumin for 3 min and chased in the presence of CSF-1 for 30 min at 37℃. The intensity of DQ-ovalbumin per pixel for 25 cells was analysed using Metamorph software. Each data-point represents one BMM cell. The mean is shown for each data-set. Data were analysed by unpaired two tail t-test. *** $P< 0.001$. NS = not significant.

monocytes and immature dendritic cells express high levels of SNX1 and SNX5 transcripts (Su et al., 2004) coinciding with their high macropinocytic activities. Our previous studies using cell lines showed that SNX5 is a molecular component of the macropinocytosis pathway (Lim et al., 2008) and that macropinocytic activity is increased when SNX5 levels are raised (Lim et al., 2008). Here we have extended these earlier findings and shown that SNX5 is a key regulator of macropinocytosis in primary macrophages. Depletion of SNX5 resulted in a dramatic reduction in macropinosome biogenesis and, moreover, resulted in a substantial reduction in antigen uptake and processing by primary macrophages, highlighting the importance of this sorting nexin and the macropinocytosis pathway in antigen presentation. The identification of SNX5 as a key regulator of the macropinocytic pathway of antigen presenting cells is an important finding as it provides a potential strategy to perturb macropinocytosis selectively *in vivo* and to analyze the biological relevance of this endocytic pathway in a range of primary specialized cells.

Macropinosomes were identified in this study using 70 kDa dextran as a fluid-phase marker. 70 kDa dextran is expected to label predominantly macropinosomes due to size constraints of entry into endocytic structures. The majority of 70 kDa dextran labelled intracellular structures by macrophages were >500 nm in diameter and the formation of these dextran labelled structures was inhibited in the presence of the macropinosome selective inhibitor, amiloride, confirming their identity. Another advantage of using the large sized 70 kDa dextran is the low level of content mixing between "older" and "newer" macropinosomes (Berthiaume et al., 1995), thereby restricting the labelling to newly-formed macropinosomes.

By generating specific antibodies to mouse sorting nexins, we have shown that endogenous SNX1 and SNX5, along with EEA1, are juxtaposed on the same newly formed macropinosome in primary macrophages. In addition endogenous SNX1 and SNX5 were shown to interact by co-immunoprecipitation, a finding consistent with previous studies that demonstrated an interaction between overexpressed exogenous SNX1 and SNX5 (Liu et al., 2006). Importantly, the studies performed here have revealed an interaction between these sorting nexins under physiological conditions in primary cells. It is likely that SNX1 and SNX5 are recruited to newly emerging macropinosomes through interaction between their PX domains and PI(3)*P* and/or PI(3,4)P_2. High levels of sorting nexins have been shown to tubulate membranes *in vitro* and drive tubulation *in vivo* (Carlton et al., 2004). Notably tubules emanating from maturing macropinosomes have been shown to label with GPF-SNX5 in HEK293 cells (Kerr et al., 2006), and we have also detected both SNX1 and SNX5 on tubular cytoplasmic structures in macrophages (unpublished data), findings consistent with the behaviour of these sorting nexins in cultured cells. Thus the behaviour of the endogenous SNXs in primary macrophages parallels their reported activity in overexpressing cultured cells.

Using a miRNA based silencing system, we have shown that depletion of SNX5 resulted in decreased macropinosome biogenesis in bone marrow-derived macrophages. This was verified using 2 different miRNA target sequences for SNX5, reducing the possibility of off-target effects. SNX5 was depleted at the progenitor stem cell stage and SNX5 depleted stem cells then differentiated into macrophages. It is possible that a deficiency of SNX5 could result in perturbation of macropinosomes as well as general endosomal transport pathways, given the potential role of SNX5 also in retromer function (Wassmer et al., 2007). However, the differentiation of phenotypically normal macrophages from SNX5-depleted stem cells would argue that general endosomal transport pathways, including those dependent on retromer, remained intact. Furthermore, deficiency of SNX5 did not affect size of macrophages or the level of surface marker F4/80, and in addition SNX5 deficiency had no effect on transferrin receptor endocytosis in mouse NIH 3T3 cells (unpublished data). Taken together, these data indicate a selective role for SNX5 associated with macropinosome biogenesis.

In contrast to the findings for SNX5, the absence of SNX1 did not affect macropinocytosis biogenesis or antigen uptake. As SNX5 was localised to macropinosomes in the absence of SNX1, membrane recruitment and function of SNX5 was independent of SNX1. We have previously shown that SNX5 can be recruited to the plasma membrane of EGF stimulated cells in the absence of SNX1 (Merino-Trigo et al., 2004) and the findings here concur that SNX5 has a role independent of SNX1 in macropinosome biogenesis. We have also previously demonstrated that SNX5 does not form a homodimer (Kerr et al., 2006), and given the dimerization properties of BAR domain proteins, is therefore likely to exist as heterodimers with SNX1 and also possibly other sorting nexins such as SNX2 which has 63% amino acid sequence identity to SNX1 (Rojas et al., 2007). Regardless, our data clearly show the SNX1-independent role of SNX5 in membrane recruitment and macropinosome biogenesis.

How might SNX5 regulate macropinocytosis in primary macrophages? The presence of the BAR domain can regulate membrane curvature (Carlton et al., 2004; Peter et al., 2004) and the BAR domain of SNX5 may be a key factor in orchestrating macropinosome formation. Following phosphoinositide dependent recruitment, SNX5 complexes may distort the plasma membrane of macrophages to subsequently form a macropinosome. The finding that depletion of SNX5 not only reduced the number, but also the size, of macropinosomes in BMM supports a role for SNX5 in defining the curvature of budding process. Also, given the potential role of SNX5 in tubulation and maturation of fully formed macropinosomes (Kerr et al., 2006), SNX5 may have multiple roles in macropinocytosis in macrophages, firstly in their biogenesis at the plasma membrane and secondly by contributing to the tubulation and maturation process of fully formed macropinosomes.

To date, the importance of macropinocytosis in antigen presentation *in vivo* has only been investigated using broad-based drug strategies such as amiloride, Sanglifehrin A or rapamycin, agents (Hackstein et al., 2007; Hackstein et al., 2002; von Delwig et al., 2006). However, *in vivo* application of these drugs is not specific. Strategies are required to selectively manipulate macropinocytosis in the whole animal system. This study identifying the role of SNX5 as a regulatory component of macropinocytosis in antigen presenting cells could therefore provide a more specific approach to determine the effect of inhibiting macropinocytosis on the immune system *in vivo*.

Materials and Methods

Antibodies and reagents

CSF-1 was purchased from Gibco (USA). Human auto-antibodies to EEA1 (Mu et al., 1995) have been described. Rat anti-mouse CD16/CD32 (Mouse BD Fc Block™) and rat anti-mouse LAMP-1 was purchased from BD Bioscience (USA). Horse-radish peroxidase (HRP)-conjugated swine anti-rabbit IgG and

rabbit anti-mouse IgG were from DAKO Corporation (Denmark). Mouse monoclonal anti-bovine α-tubulin, goat anti-human IgG Alexa Fluor™ 647, goat anti-rabbit IgG Alexa Fluor™ 568, goat anti-rabbit IgG Alexa Fluor™ 647 and goat anti-rat IgG Alexa Fluor™ 488, lysine-fixable TxR-conjugated 70 kDa dextran, fluorescein isothiocynate (FITC)-conjugated 70 kDa dextran, Alexa Fluor™ 555-conjugated ovalbumin and DQ-ovalbumin were purchased from Molecular Probes (USA).

Recombinant DNA constructs

cDNA was obtained from mouse testis mRNA of BALB/c mice by reverse transcription PCR. The full length cDNA of SNX1 was amplified from mouse testis cDNA and the resulting PCR product was cloned into *Eco*RI/*Xma*I sites of pEGFP-C1 (Clontech, USA) to generate pEGFP-C1-SNX1 construct. To generate pEGFP-C1-SNX5, the full length cDNA of SNX5 was amplified from mouse testis cDNA and the resulting PCR product was cloned into *Kpn*I/*Bam*HI sites of pEGFP-C1.

cDNAs or miRNA were cloned into pDC315 (Microbix Biosystems, Canada) for generating recombinant adenovirus (rADV). To generate pDC315-GFP-SNX5, full length cDNA encoding SNX5 inserted at the C-terminal GFP was amplified from pEGFP-C1-SNX5 and cloned into *Bam*HI site of pDC315. For pDC315-GFP-miRNA constructs, control miRNA, miRNA-1.4 and miRNA-2.4 were amplified from pcDNA™ 6.2GW/EmGFP control miRNA, pcDNA™ 6.2GW/EmGFP-miRNA-1.4 and pcDNA™ 6.2GW/EmGFP-miRNA-2.4, respectively. The resulting miRNA target sequences with the GFP reporter gene were cloned into *Eco*RI/*Sal*I sites of pDC315. All constructs were verified by DNA sequencing.

Generation of antibodies specific for mouse SNX1 and SNX5

Anti-SNX1 antibodies

A region corresponding to the N-terminal 108 residue of mouse SNX1 ($SNX1_{1–108}$) was amplified using mouse testis cDNA as template. $SNX1_{1–108}$ was then cloned into the *Eco*RI/*Xho*I sites of pGEX-6P3 vector. The GST fusion protein was expressed and purified from in *E. coli* BL-21 cells using a Glutathione Sepharose 4B (GE Healthcare, UK) column and dialysed against PBS overnight. GST-$SNX_{1–108}$ was injected subcutaneously into New Zealand white rabbits. Two additional boost injections were given 27 days and 48 days after the initial immunisation. Terminal bleed was carried out 60 days after the initial immunisation. All immunisation procedures were performed by Millipore (USA). Antibodies were affinity purified from the terminal bleed serum using a column of $SNX1_{1–108}$ protein conjugated to CNBr-activated Sepharose 4B beads (GE Healthcare, UK) according to manufacturer's instructions. Bound antibodies were subjected to alternate high and low salt washes prior to low-pH elution. Affinity-purified antibodies reacted by immunoblotting with a 88 kDa GFP-full length SNX1 fusion protein from transfected NIH3T3 cells, in addition to the predicted endogenous ~70 kDa SNX1 protein (supplementary material Fig. S3A). The affinity-purified antibodies co-localised with the punctate staining pattern of GFP-SNX1 and detected punctate structures in untransfected NIH3T3 cells, which correspond to the expected location of endogenous SNX1 (supplementary material Fig. S3C), confirming that the antibodies are specific for SNX1.

Anti-SNX5 antibodies

A synthetic peptide corresponding to the N-terminal 35 residues of mouse SNX5 ($SNX5_{1–35}$), with an additional cysteine residue at the C-terminus was synthesised (Research Transfer Facility, BIO21 Institute). Sequence of peptide is: MAAVPELLEQQEEDRSKLRSVSVDLNVDPSLQIDIC. $SNX5_{1–35}$ peptide was directly injected subcutaneously into New Zealand white rabbit. Three additional boost injections were given 21, 42 and 63 days after the initial immunisation. A terminal bleed was carried out 99 days after the initial immunisation. Immunisation was performed by Invitrogen (USA). Antibodies were affinity purified from the terminal bleed serum using a column of $SNX5_{1–35}$ peptide conjugated to SulfoLink Coupling Gel (Pierce, USA) according to manufacturer's instructions. Affinity-purified antibodies recognised the expected size of the endogenous SNX5 (~ 50 kDa) and also a ~ 76 kDa band which corresponded to the size of GFP-SNX5 (supplementary material Fig. S3B). The affinity-purified antibodies stained punctate structures in untransfected NIH3T3 cells and co-localised with punctate staining pattern of GFP-SNX5 of transfected NIH3T3, demonstrating specificity for SNX5 (supplementary material Fig. S3D).

Cell culture and transfection

L-cells were maintained in RPMI (Invitrogen, USA) supplemented with 10% (v/v) foetal calf serum (JRH, Australia), 100 units/ml penicillin, 100 µg/ml streptomycin and 2 mM L-glutamine. NIH3T3 and 293 cells were maintained as monolayers in DMEM (Invitrogen, USA) supplemented with 10% (v/v) foetal calf serum, 100 units/ml penicillin, 100 µg/ml streptomycin and 2 mM L-glutamine. All cells were cultured in a humidified 37℃ incubator with 10% CO_2. Transient transfections of cells with vector-based constructs were performed using Fugene 6 transfection reagent (Roche, USA) according to the manufacturer's instructions. Cells were incubated for 48–96 hours, as indicated, to allow expression of construct.

SNX1$^{-/-}$ mice

SNX1$^{-/-}$ mice were purchased from Mutant Mouse Regional Resource Centres (USA) and have been previously described (Schwarz et al., 2002). Litters of weaned pups were genotyped as described (Schwarz et al., 2002) with annealing temperature for the PCR reactions set at 59.3℃.

RNA interference

For knockdown of SNX5 expression in cells, a miRNA system was employed. The following primer pairs were designed using the Invitrogen BLOCK-iT™ RNAi Designer (https://rnaidesigner.invitrogen.com/rnaiexpress), annealed and cloned into pcDNA™ 6.2GW/EmGFP-miRNA expression vector which contains a GFP expression cassette.

miRNA-1: 5′-TGCTGTTTAGCACAGGAATCCTTGATGTTTTGGCCAC-TGACTGACATCAAGGACCTGTGCTAAA-3′ and 5′-CCTGTTTAGCACAGG-TCCTTGATGTCAGTCAGTGGCCAAAACATCAAGGATTCCTGTGCTAAAC-3′, miRNA-2: 5′-TGCTGTGCACTGTAAACTTGACCTTAGTTTTGGCCACTG-ACTGACTAAGGTCATTTACAGTGCA-3′ and 5′-CCTGTGCACTGTAAATG-ACCTTAGTCAGTCAGTGGCCAAAACTAAGGTCAAGTTTACAGTGCAC-3′ and control miRNA that has no homology to any known mouse gene.

pcDNA™ 6.2GW/EmGFP-miRNA-1 was digested using *Bam*HI and *Xho*I restriction enzymes to obtain miRNA-1 insert. The resulting 152 bp fragment was cloned into the *Bgl*II/*Xho*I sites of a pcDNA™ 6.2GW/EmGFP-miRNA-1 from a separate restriction enzyme digest generating pcDNA™ 6.2GW/EmGFP-miRNA-1.2 (contains 2 tandem copies of miRNA-1). pcDNA™ 6.2GW/EmGFP-miRNA-1.2 was then digested using *Bam*HI and *Xho*I restriction enzymes to obtain miRNA-1.2 insert. The resulting 291 bp fragment was cloned into the *Bgl*II/*Xho*I sites of a pcDNA™ 6.2GW/EmGFP-miRNA-1.2 from a separate restriction enzyme digest thereby generating pcDNA™ 6.2GW/EmGFP-miRNA-1.4 (contains 4 tandem copies of miRNA-1). The same cloning strategy was used to obtain miRNA-2.4.

Isolation of primary peritoneal and bone marrow-derived macrophages

Eight to ten week old BALB/c mice were killed by CO_2 asphyxiation in accordance with animal ethic guidelines.

To isolate primary peritoneal macrophages, 9 ml of ice-cold serum-free RPMI (Invitrogen, USA) was injected into the peritoneal cavity. Macrophages were liberated by massage and the peritoneal cells collected back into the syringe. Cells were pelleted at 394 *g* for 5 min and resuspended in 5 ml of 0.9% (w/v) NH_4Cl for 5 min at 37℃ to lyse contaminating red blood cells. Cold 0.1% (w/v) BSA/PBS (5 ml) was then added and cells were collected by centrifugation. Cells were resuspended and cultured overnight in RPMI supplemented with 10% (v/v) foetal calf serum, 100 units/ml penicillin, 100 µg/ml streptomycin and 2 mM L-glutamine in a humidified 37℃ incubator with 10% CO_2. Cells were then washed twice in serum-free RPMI to remove any non-adherent cells.

To isolate bone marrow-derived macrophages, cells were obtained from the femurs and tibias of mice. Red blood cells were then lysed and cells pelleted by centrifugation. Cells were resuspended in complete bone marrow medium (RPMI supplemented with 15% (v/v) FCS, 20% (v/v) L-cell conditioned medium, 100 units/ml penicillin, 100 µg/ml streptomycin and 2 mM L-glutamine), seeded onto a tissue culture dish and grown in a humidified 37℃ incubator with 10% CO_2 overnight. The medium containing the progenitor bone marrow stem cells were obtained the next day and differentiated into bone marrow-derived macrophages by culturing in the presence of CSF-1 (from the L-cell conditioned medium) for 5–7 days in a humidified 37℃ incubator with 10% CO_2.

Recombinant adenovirus production and transduction

Recombinant adenovirus (rADV) shuttle plasmid containing the gene of interest and rADV genomic plasmid, pBHGloxΔE1,3Cre (Microbix, Canada) containing a modified adenovirus type-5 genome, were co-transfected into 293 cells using Fugene 6 according to manufacturer's instructions. A single viral colony (rADV plaque in agarose) was isolated and amplified in 293 cells. Virus harvested from the 293 cells was titrated in NIH3T3 cells by scoring for the expression of the fluorescent GFP tag. Each batch of recombinant virus was analysed for the expression of the construct by immunoblotting and immunofluorescence analysis. Aliquots of virus were stored at −80℃.

For transduction of NIH3T3 cells, cells were incubated with rADV in the presence of serum-free DMEM at a multiplicity of infection (MOI) of 10–20 at 37℃, 10% CO_2 for 2 hours with shaking every 15 min. The medium containing rADV was then removed and replaced with complete DMEM and cells were grown in a humidified 10% CO_2 atmosphere at 37℃ as indicated.

For transduction of peritoneal macrophages, cells were incubated with rADV at a MOI of 1 in the presence of complete RPMI in a humidified 10% CO_2 atmosphere at 37℃ overnight.

For transduction of progenitor bone marrow cells, cells were incubated with rADV at a MOI of 0.5–2 in the presence of complete bone marrow medium in a humidified 10% CO_2 atmosphere at 37℃ for 24 hours. Cells were then pelleted at

394 *g* for 5 min, medium containing rADV removed and replaced with fresh complete bone marrow medium and cells grown for an additional 48 hours in complete bone marrow medium.

Cell sorting

GFP-positive cells were sorted using a FACSAria Cell Sorter at the ImmunoID Flow Cytometry Facility (Department of Microbiology and Immunology, University of Melbourne).

5-(N-ethyl-N-isopropyl) amiloride treatment

Macrophages were pre-treated with 100 μM of 5-(N-ethyl-N-isopropyl) amiloride (Sigma, Israel) diluted in serum-free RPMI medium at 37℃ for 30 min prior to dextran uptake.

Fluid phase uptake assays

Peritoneal macrophages from BALB/c mice were incubated with 500 μg/ml of lysine-fixable, FITC-conjugated 70 kDa dextran for 15 min at 37℃ in serum-free RPMI. For bone marrow-derived macrophages, cells were firstly cultured overnight in the absence of CSF-1 to render macrophages quiescent. Then, macrophages were incubated with 500 μg/ml of fluorescently-conjugated 70 kDa dextran, or 50 μg/ml of Alexa Fluor™ 555-conjugated ovalbumin, in the presence of 50 ng/ml of CSF-1 in serum-free RPMI at 37℃. Following the incubation cells were placed on ice for 5 min to inhibit uptake of dextran/ovalbumin and cells and then washed with cold complete RPMI and PBS. Control incubations were also performed on ice. Cells were fixed and processed for immunofluorescence.

Pulse-chase DQ-ovalbumin

Bone marrow-derived macrophages were cultured overnight in the absence of CSF-1. The cells were then pulsed with 50 μg/ml of DQ-ovalbumin for 3 min at 37℃ in the presence of 50 ng/ml of CSF-1 diluted in serum-free RPMI. Cells were washed with PBS and the chase was performed in serum-free RPMI in the presence of CSF-1 for 30 min at 37℃. The chase was terminated by incubation on ice for 5 min. As control, macrophages were incubated with DQ-ovalbumin on ice for 30 min. Cells were fixed and processed for immunofluorescence.

Indirect immunofluorescence and microscopy

Cells were fixed in paraformaldehyde, permeabilised, and processed for immunofluorescence as previously described (Kjer-Nielsen et al., 1999). For macrophage staining, an additional blocking step using Mouse BD Fc Block™ at room temperature for 30 min was performed prior to the addition of primary antibodies. For LAMP-1 staining, Mouse BD Fc Block™ was omitted and cells fixed in ice-cold methanol, instead of paraformaldehyde, for 5 min at −20℃ prior to blocking and staining. Cells were examined using a Leica TCS SP2 system and Leica Confocal Software version 2.61. For multi-colour labelling, images were collected independently. Images were analysed using Metamorph Version 7.5.6.0 software.

Immunoprecipitation

Cells were harvested with a cell scraper, washed twice in cold PBS and lysed in 500 μl cell lysis solution (1% (v/v) IGEPAL CA-630 (Sigma, USA), containing Complete™ protease inhibitor (Roche, Germany), PBS), for 45 min on ice. Cellular debris was removed by centrifugation. Antibodies were added to the clarified supernatant at a final concentration of 4 μg/ml and the mixture rotated at 4℃ overnight. The following day, 4% (v/v) Protein G Sepharose™ 4 Fast Flow (GE Healthcare Life Sciences, Sweden) was added and the mixture rotated for 1 hour. Beads were collected by centrifugation and washed twice for 10 min at 4℃ in cold lysis solution prior to a final wash in cold PBS. Beads were then collected by centrifugation and bound antibody complexes eluted from the beads by boiling in 4× reducing sample buffer (200 mM Tris-HCl, 8% (w/v) SDS, 0.4% (w/v) Bromophenol Blue, 40% (v/v) glycerol, 400 mM DTT) for 5 min.

Immunoblotting

Cells were lysed directly by boiling for 5 min in 2× reducing sample buffer (100 mM Tris-HCl, 4% (w/v) SDS, 0.2% (w/v) Bromophenol Blue, 20% (v/v) glycerol, 200 mM DTT). Proteins were resolved in a 10% NuPAGE® gel (Invitrogen, USA) and then transferred onto Immobilon-P PVDF membranes (Millipore, USA) at 30 V overnight at 4℃, according to munfacturer's instructions. Membranes were dried and incubated with primary antibodies diluted in 1% (w/v) BSA dissolved in PBS-Tween (0.1(v/v) % Tween-20/PBS) for 1 hour then washed three times for 5 min each in PBS-Tween. Membranes were then incubated with HRP-conjugated secondary antibodies for 1 h and washed as before. Bound antibodies were detected using chemiluminescence and images captured using Gel-ProTM Analyser version 4.5 software. Bound antibodies were stripped from the membrane using PVDF membrane stripping buffer (25 mM glycine, 1% (w/v) SDS, PBS, pH 2) as necessary. Membranes were then washed and blocked, as previously, and incubated with different primary antibodies.

Statistical analysis

The unpaired two-tailed Student *t* test was used to determine statistical significance. A *p*-value of <0.05 (*) was considered as significant, *p*-value of <0.01(**) was highly significant and $P<0.001$ (***) was very highly significant. The absence of a *p* value indicates the differences were not significant.

Acknowledgements

This work was supported by funding from the National Health and Medical Research Council (NHMRC) of Australia (ID566727). RDT was supported by an NHMRC Senior Research Fellowship (511042). JPL was supported by an Endeavour International Postgraduate Research Scholarship and Melbourne International Research Scholarship.

Competing Interests

The authors have no competing interests to declare.

References

Amyere, M., Payrastre, B., Krause, U., Van Der Smissen, P., Veithen, A. and Courtoy, P. J. (2000). Constitutive macropinocytosis in oncogene-transformed fibroblasts depends on sequential permanent activation of phosphoinositide 3-kinase and phospholipase C. *Mol. Biol. Cell* **11**, 3453-3467.

Anzinger, J. J., Chang, J., Xu, Q., Barthwal, M. K., Bohnacker, T., Wymann, M. P. and Kruth, H. S. (2012). Murine bone marrow-derived macrophages differentiated with GM-CSF become foam cells by PI3Kγ-dependent fluid-phase pinocytosis of native LDL. *J. Lipid Res.* **53**, 34-42.

Araki, N., Johnson, M. T. and Swanson, J. A. (1996). A role for phosphoinositide 3-kinase in the completion of macropinocytosis and phagocytosis by macrophages. *J. Cell Biol.* **135**, 1249-1260.

Berthiaume, E. P., Medina, C. and Swanson, J. A. (1995). Molecular size-fractionation during endocytosis in macrophages. *J. Cell Biol.* **129**, 989-998.

Bryant, D. M., Kerr, M. C., Hammond, L. A., Joseph, S. R., Mostov, K. E., Teasdale, R. D. and Stow, J. L. (2007). EGF induces macropinocytosis and SNX1-modulated recycling of E-cadherin. *J. Cell Sci.* **120**, 1818-1828.

Carlton, J., Bujny, M., Peter, B. J., Oorschot, V. M., Rutherford, A., Mellor, H., Klumperman, J., McMahon, H. T. and Cullen, P. J. (2004). Sorting nexin-1 mediates tubular endosome-to-TGN transport through coincidence sensing of high-curvature membranes and 3-phosphoinositides. *Curr. Biol.* **14**, 1791-1800.

Carlton, J., Bujny, M., Rutherford, A. and Cullen, P. (2005). Sorting nexins–unifying trends and new perspectives. *Traffic* **6**, 75-82.

Carpentier, J. L., Lew, D. P., Paccaud, J. P., Gil, R., Iacopetta, B., Kazatchkine, M., Stendahl, O. and Pozzan, T. (1991). Internalization pathway of C3b receptors in human neutrophils and its transmodulation by chemoattractant receptors stimulation. *Cell Regul.* **2**, 41-55.

Clague, M. J., Thorpe, C. and Jones, A. T. (1995). Phosphatidylinositol 3-kinase regulation of fluid phase endocytosis. *FEBS Lett.* **367**, 272-274.

Cullen, P. J. (2008). Endosomal sorting and signalling: an emerging role for sorting nexins. *Nat. Rev. Mol. Cell Biol.* **9**, 574-582.

Daro, E., Pulendran, B., Brasel, K., Teepe, M., Pettit, D., Lynch, D. H., Vremec, D., Robb, L., Shortman, K., McKenna, H. J. et al. (2000). Polyethylene glycol-modified GM-CSF expands CD11b(high)CD11c(high) but notCD11b(low) CD11c(high) murine dendritic cells *in vivo*: a comparative analysis with Flt3 ligand. *J. Immunol.* **165**, 49-58.

Dharmawardhane, S., Schürmann, A., Sells, M. A., Chernoff, J., Schmid, S. L. and Bokoch, G. M. (2000). Regulation of macropinocytosis by p21-activated kinase-1. *Mol. Biol. Cell* **11**, 3341-3352.

Eckfeldt, C. E., Mendenhall, E. M., Flynn, C. M., Wang, T. F., Pickart, M. A., Grindle, S. M., Ekker, S. C. and Verfaillie, C. M. (2005). Functional analysis of human hematopoietic stem cell gene expression using zebrafish. *PLoS Biol.* **3**, e254.

Hackstein, H., Taner, T., Logar, A. J. and Thomson, A. W. (2002). Rapamycin inhibits macropinocytosis and mannose receptor-mediated endocytosis by bone marrow-derived dendritic cells. *Blood* **100**, 1084-1087.

Hackstein, H., Steinschulte, C., Fiedel, S., Eisele, A., Rathke, V., Stadlbauer, T., Taner, T., Thomson, A. W., Tillmanns, H., Bein, G. et al. (2007). Sanglifehrin a blocks key dendritic cell functions *in vivo* and promotes long-term allograft survival together with low-dose CsA. *Am. J. Transplant.* **7**, 789-798.

Haigler, H. T., McKanna, J. A. and Cohen, S. (1979). Rapid stimulation of pinocytosis in human carcinoma cells A-431 by epidermal growth factor. *J. Cell Biol.* **83**, 82-90.

Hewlett, L. J., Prescott, A. R. and Watts, C. (1994). The coated pit and macropinocytic pathways serve distinct endosome populations. *J. Cell Biol.* **124**, 689-703.

Kerr, M. C., Lindsay, M. R., Luetterforst, R., Hamilton, N., Simpson, F., Parton, R. G., Gleeson, P. A. and Teasdale, R. D. (2006). Visualisation of macropinosome maturation by the recruitment of sorting nexins. *J. Cell Sci.* **119**, 3967-3980.

Kerr, M. C., Wang, J. T., Castro, N. A., Hamilton, N. A., Town, L., Brown, D. L., Meunier, F. A., Brown, N. F., Stow, J. L. and Teasdale, R. D. (2010). Inhibition of the PtdIns(5) kinase PIKfyve disrupts intracellular replication of Salmonella. *EMBO J.* **29**, 1331-1347.

Kjer-Nielsen, L., van Vliet, C., Erlich, R., Toh, B. H. and Gleeson, P. A. (1999). The Golgi-targeting sequence of the peripheral membrane protein p230. *J. Cell Sci.* **112**, 1645-1654.

Koivusalo, M., Welch, C., Hayashi, H., Scott, C. C., Kim, M., Alexander, T., Touret, N., Hahn, K. M. and Grinstein, S. (2010). Amiloride inhibits macropinocytosis by lowering submembranous pH and preventing Rac1 and Cdc42 signaling. *J. Cell Biol.* **188**, 547-563.

Lim, J. P. and Gleeson, P. A. (2011). Macropinocytosis: an endocytic pathway for internalising large gulps. *Immunol. Cell Biol.* **89**, 836-843.

Lim, J. P., Wang, J. T., Kerr, M. C., Teasdale, R. D. and Gleeson, P. A. (2008). A role for SNX5 in the regulation of macropinocytosis. *BMC Cell Biol.* **9**, 58.

Liu, H., Liu, Z. Q., Chen, C. X., Magill, S., Jiang, Y. and Liu, Y. J. (2006). Inhibitory regulation of EGF receptor degradation by sorting nexin 5. *Biochem. Biophys. Res. Commun.* **342**, 537-546.

Merino-Trigo, A., Kerr, M. C., Houghton, F., Lindberg, A., Mitchell, C., Teasdale, R. D. and Gleeson, P. A. (2004). Sorting nexin 5 is localized to a subdomain of the early endosomes and is recruited to the plasma membrane following EGF stimulation. *J. Cell Sci.* **117**, 6413-6424.

Mu, F.-T., Callaghan, J. M., Steele-Mortimer, O., Stenmark, H., Parton, R. G., Campbell, P. L., McCluskey, J., Yeo, J.-P., Tock, E. P. C. and Toh, B.-H. (1995). EEA1, an early endosome-associated protein. EEA1 is a conserved α-helical peripheral membrane protein flanked by cysteine "fingers" and contains a calmodulin-binding IQ motif. *J. Biol. Chem.* **270**, 13503-13511.

Norbury, C. C., Hewlett, L. J., Prescott, A. R., Shastri, N. and Watts, C. (1995). Class I MHC presentation of exogenous soluble antigen via macropinocytosis in bone marrow macrophages. *Immunity* **3**, 783-791.

Norbury, C. C., Chambers, B. J., Prescott, A. R., Ljunggren, H. G. and Watts, C. (1997). Constitutive macropinocytosis allows TAP-dependent major histocompatibility complex class I presentation of exogenous soluble antigen by bone marrow-derived dendritic cells. *Eur. J. Immunol.* **27**, 280-288.

Peter, B. J., Kent, H. M., Mills, I. G., Vallis, Y., Butler, P. J., Evans, P. R. and McMahon, H. T. (2004). BAR domains as sensors of membrane curvature: the amphiphysin BAR structure. *Science* **303**, 495-499.

Racoosin, E. L. and Swanson, J. A. (1989). Macrophage colony-stimulating factor (rM-CSF) stimulates pinocytosis in bone marrow-derived macrophages. *J. Exp. Med.* **170**, 1635-1648.

Rojas, R., Kametaka, S., Haft, C. R. and Bonifacino, J. S. (2007). Interchangeable but essential functions of SNX1 and SNX2 in the association of retromer with endosomes and the trafficking of mannose 6-phosphate receptors. *Mol. Cell. Biol.* **27**, 1112-1124.

Sallusto, F., Cella, M., Danieli, C. and Lanzavecchia, A. (1995). Dendritic cells use macropinocytosis and the mannose receptor to concentrate macromolecules in the major histocompatibility complex class II compartment: downregulation by cytokines and bacterial products. *J. Exp. Med.* **182**, 389-400.

Santambrogio, L., Sato, A. K., Carven, G. J., Belyanskaya, S. L., Strominger, J. L. and Stern, L. J. (1999). Extracellular antigen processing and presentation by immature dendritic cells. *Proc. Natl. Acad. Sci. USA* **96**, 15056-15061.

Schwarz, D. G., Griffin, C. T., Schneider, E. A., Yee, D. and Magnuson, T. (2002). Genetic analysis of sorting nexins 1 and 2 reveals a redundant and essential function in mice. *Mol. Biol. Cell* **13**, 3588-3600.

Steinman, R. M., Brodie, S. E. and Cohn, Z. A. (1976). Membrane flow during pinocytosis. A stereologic analysis. *J. Cell Biol.* **68**, 665-687.

Su, A. I., Wiltshire, T., Batalov, S., Lapp, H., Ching, K. A., Block, D., Zhang, J., Soden, R., Hayakawa, M., Kreiman, G. et al. (2004). A gene atlas of the mouse and human protein-encoding transcriptomes. *Proc. Natl. Acad. Sci. USA* **101**, 6062-6067.

Swanson, J. A. (1989). Phorbol esters stimulate macropinocytosis and solute flow through macrophages. *J. Cell Sci.* **94**, 135-142.

Swanson, J. A. and Watts, C. (1995). Macropinocytosis. *Trends Cell Biol.* **5**, 424-428.

Teasdale, R. D., Loci, D., Houghton, F., Karlsson, L. and Gleeson, P. A. (2001). A large family of endosome-localized proteins related to sorting nexin 1. *Biochem. J.* **358**, 7-16.

Tsang, A. W., Oestergaard, K., Myers, J. T. and Swanson, J. A. (2000). Altered membrane trafficking in activated bone marrow-derived macrophages. *J. Leukoc. Biol.* **68**, 487-494.

von Delwig, A., Hilkens, C. M., Altmann, D. M., Holmdahl, R., Isaacs, J. D., Harding, C. V., Robertson, H., McKie, N. and Robinson, J. H. (2006). Inhibition of macropinocytosis blocks antigen presentation of type II collagen *in vitro* and *in vivo* in HLA-DR1 transgenic mice. *Arthritis Res. Ther.* **8**, R93.

Wang, J. T., Kerr, M. C., Karunaratne, S., Jeanes, A., Yap, A. S. and Teasdale, R. D. (2010). The SNX-PX-BAR family in macropinocytosis: the regulation of macropinosome formation by SNX-PX-BAR proteins. *PLoS ONE* **5**, e13763.

Wassmer, T., Attar, N., Bujny, M. V., Oakley, J., Traer, C. J. and Cullen, P. J. (2007). A loss-of-function screen reveals SNX5 and SNX6 as potential components of the mammalian retromer. *J. Cell Sci.* **120**, 45-54.

Wassmer, T., Attar, N., Harterink, M., van Weering, J. R., Traer, C. J., Oakley, J., Goud, B., Stephens, D. J., Verkade, P., Korswagen, H. C. et al. (2009). The retromer coat complex coordinates endosomal sorting and dynein-mediated transport, with carrier recognition by the trans-Golgi network. *Dev. Cell* **17**, 110-122.

West, M. A., Bretscher, M. S. and Watts, C. (1989). Distinct endocytotic pathways in epidermal growth factor-stimulated human carcinoma A431 cells. *J. Cell Biol.* **109**, 2731-2739.

Worby, C. A. and Dixon, J. E. (2002). Sorting out the cellular functions of sorting nexins. *Nat. Rev. Mol. Cell Biol.* **3**, 919-931.

Xu, Y., Seet, L. F., Hanson, B. and Hong, W. (2001). The Phox homology (PX) domain, a new player in phosphoinositide signalling. *Biochem. J.* **360**, 513-530.

Yoshida, S., Hoppe, A. D., Araki, N. and Swanson, J. A. (2009). Sequential signaling in plasma-membrane domains during macropinosome formation in macrophages. *J. Cell Sci.* **122**, 3250-3261.